

# In Silico Structural Characterizations of Pyrazinamidase Variants from Various Species of *Mycobacterium*

Arasu Prabhavadhni, Biswajit Gorai, Palaniappan L Visalakshi and Thirunavukkarasu Sivaraman\*

Structural Biology Lab, Anusandhan Kendra, School of Chemical and Biotechnology,  
SASTRA University, Thanjavur – 613401, Tamil Nadu, India.

## Abstract

Tuberculosis is a chronic disease caused by various strains of *Mycobacterium*, primarily by *Mycobacterium tuberculosis*, which usually attacks lungs. The enzyme fatty acid synthase is essential for survival of the *Mycobacteria* and hence it has become a potential chemotherapeutic target. Pyrazinamide, a prodrug, in combination with the antibiotics is being used as a paradoxical frontline drug against the infections and the enzyme pyrazinamidase present in the bacteria converts the prodrug into pyrazinoic acid, an inhibitor to fatty acid synthase. However, six species of mycobacterium such as *M. bovis*, *M. kansasii*, *M. avium*, *M. smegmatis*, *M. abscessus* and *M. marinum* are resistant to pyrazinamide due to the random mutations in the primary sequences of the pyrazinamidases. In this study, computational rationalization for the differential binding affinities of pyrazinamide on the binding grooves of pyrazinamidase variants from various species of *Mycobacterium* could be derived in order to bring an insight on the mechanisms behind the pyrazinamide-resistance of the pyrazinamidases. In these contexts, we have herein demonstrated that absence or ill-formed 'GATE' regions of pyrazinamidases may act as probable structural factors for the differential binding affinities of the pyrazinamidase variants towards the interaction with pyrazinamide (PZA) and as well PZA-resistant properties of the enzymes.

**Keywords:** Binding affinity, 'GATE' region, Fatty acid synthase, *Mycobacterium tuberculosis*, Pyrazinamidase and Pyrazinamide.

## 1. INTRODUCTION

Tuberculosis (TB) is a chronic infectious disease caused by various strains of *Mycobacteria*, primarily *Mycobacterium tuberculosis*, which are multidrug-resistant (MDR) to isoniazid and rifampin, the backbone of first-line anti-tuberculosis treatment [1-3]. Pyrazinamidase is a 20.89 kDa monomer with an average length of 186 amino acids across various species of *Mycobacterium*. Pyrazinamidase (PZase), an enzyme encoded by PncA gene converts the prodrug pyrazinamide (PZA) into its active form pyrazinoic acid (POA) [4-5]. Pyrazinamide is a first line sterilizing drug in tuberculosis therapy as this drug plays a key role in shortening the duration of the chemotherapy [6,7]. Pyrazinamide diffuses into *M. tuberculosis*, where PZase converts PZA to POA and more pyrazinoic acid accumulates inside the bacillus, which inhibits the fatty acid synthase I of the organisms. Since fatty acid synthesis in bacteria is essential for cell survival, enzymes involved in this pathway are the potential targets for antimicrobial agents [8]. Six species of *Mycobacterium* such as *M. bovis*, *M. kansasii*, *M. abscessus*, *M. marinum*, *M. avium* and *M. smegmatis* are resistant to pyrazinamide due to random mutation in the PncA gene in general [9-13]. Of the six species, *M. kansasii*, *M. abscessus*, *M. marinum* and *M. smegmatis* are non-tuberculosis forms but they are capable of causing tuberculosis and pulmonary lesions when a patient is already affected by AIDS. In the present study, the mechanisms behind the resistance of above said species to pyrazinamide could be unraveled by analyzing the active sites and 'GATE' regions of the enzymes by means of computational approaches.

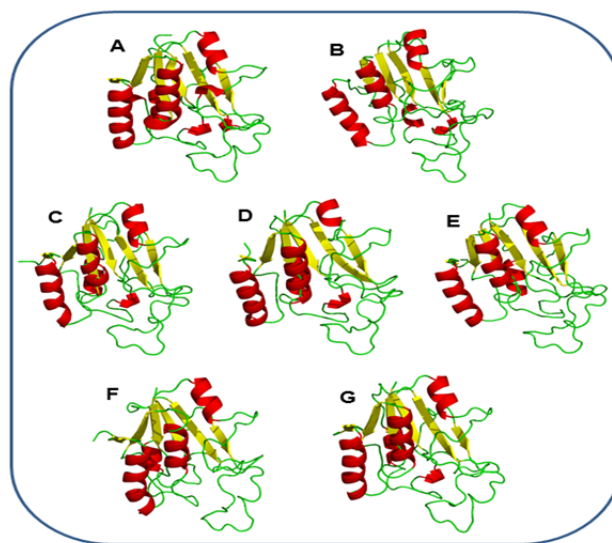


**Figure 1:** 3D structures of pyrazinamidases from A) *M. abscessus*, B) *M. avium*, C) *M. bovis*, D) *M. kansasii*, E) *M. marinum*, F) *M. smegmatis* and G) *M. tuberculosis*.

## 2. MATERIALS AND METHODS

### 2.1 Structure predictions and validations of pyrazinamidase

The crystal structure of pyrazinamidase of *M. tuberculosis* (PDB ID: 3PL1) was retrieved from PDB (<http://www.rcsb.org/>). The sequences of the PZases for the remaining six species were collected from UniProtKB/Swiss-Prot (<http://www.uniprot.org/>) using BLAST. The homology modeling of the PZase enzymes from the six different species was individually done using

Modeller9v8 [14]. Twenty structures were initially generated in each case and representative three-dimensional (3D) structure of PZase for each species could be selected on the basis of modeler convergence function value and structural parameters as calculated by using SAVES server (<http://services.mbi.ucla.edu/SAVES/>).

## 2.2 Molecular dynamics simulations

The modeled pyrazinamidases of various species of *Mycobacterium* were solvated in water and then energy minimized and simulated at 310 K using GROMACS - 4.5.4 [15]. The box type was defined as a dodecahedron. TIP3P (Transferrable Intermolecular Potential) water model [16], generic equilibrated 3-point solvent model was used. Equilibration was conducted in two phases, NVT ensemble for 200 ps and NPT ensemble for 500 ps and the system was well-equilibrated at the desired temperature and pressure. Then position restraints were released and production MD was run for 2 ns.

In order to perform molecular dynamics of PZase –PZA complexes, the topology for the ligand was collected from SwissParam (<http://www.swissparam.ch>) web service. CHARMM27 all-atom force field and TIP3P water model were used [17,18]. Pyrazinamidase models of both resistant and susceptible species of *Mycobacterium* were energy minimized in vacuum at 310 K and 373 K to obtain their global energy minima. Equilibration was conducted in two phases, NVT ensemble for 200 ps and, NPT ensemble for 500 ps and the system was well-equilibrated at the desired temperature and pressure. Then position restraints were released and production MD was run for data collection at 5ns.

## 2.3 Binding site predictions and depth analysis

Two online tools Q-Site Finder (<http://www.modelling.leeds.ac.uk/qsitefinder/>) [19] and Pocket-Finder (<http://www.modelling.leeds.ac.uk/pocketfinder/>) and an offline tool, SiteMap (Schrödinger suite software) were used to predict the binding sites of PZases. DogSiteScorer (<http://dogsite.zbh.uni-hamburg.de/>), an online tool, which was used for depth analyses of binding pockets of PZase enzymes [20].

## 2.4 Retrieval of PZA and its molecular docking studies

The pyrazinamide was taken from PubChem (<https://pubchem.ncbi.nlm.nih.gov>) and the ligand was used to generate docking complexes of PZase – PZA by using molecular docking studies. The rigid receptor-flexible ligand docking mode was employed by using the Lamarckian genetic algorithm of Autodock 4, a suite of automated docking tool [21]. The ligand in the PDB format was converted into PDBQT format (by defining the active torsion, root, end branch and branch) for setting up the ligand. The protein in the PDB format was also converted into PDBQT format by adding all hydrogen and Gasteiger charges for setting up the protein. Grid was used to specify the binding site of the PZase enzymes. Various docking

conformations of PZA were clustered and a cluster with lowest energy was chosen for further studies of the present works.

## 3. RESULTS AND DISCUSSION

### 3.1 Multiple sequence alignments and Homology modeling

Pyrazinamidase sequences from various *Mycobacterium* species were aligned using ClustalW to analyze evolutionary mutated residues, which may play crucial roles behind the PZA-resistance of pyrazinamidase of *Mycobacterium* species. However, the analyses were not straightforward as active site residues of PZase were unknown to date. Sequence from H37RV strain of *M.tuberculosis* was considered for modeling the pyrazinamidase of other species. Resistant species of *Mycobacterium* such as *M.bovis*, *M.abscessus*, *M.avium*, *M.kansasii*, *M.marinum*, and *M.smegmatis* had variation in the sequence of PncA and therefore modeled as per their unique sequence alignments. Template used for the modeling procedures was 3PL1 and percentage of identity between the template and PZase sequences from *M.bovis*, *M.kansasii*, *M.marinum*, *M.avium*, *M.smegmatis* and *M.abscessus* were 99%, 71%, 70%, 69%, 67% and 59% respectively. The 3D structures of all seven species of *Mycobacterium* are depicted in **Fig. 1** and values of root mean square deviation (RMSD) between the 3D structures of PZase from various species and template (3PL1) PZase structure were found to be 0.98 Å, 1.0 Å, 1.1 Å, 1.2 Å, 1.2 Å and 1.4 Å for PZase from *M.avium*, *M.kansasii*, *M.abscessus*, *M.smegmatis*, *M.bovis* and *M.marinum*, respectively. All the modeled 3D structures of PZases were simulated at 310 K for a dynamic timescale of 2 ns and a dynamic structure from equilibrium regions of each simulation process was selected for further studies of the present works.

### 3.2 Prediction of binding sites of PZases and molecular dockings

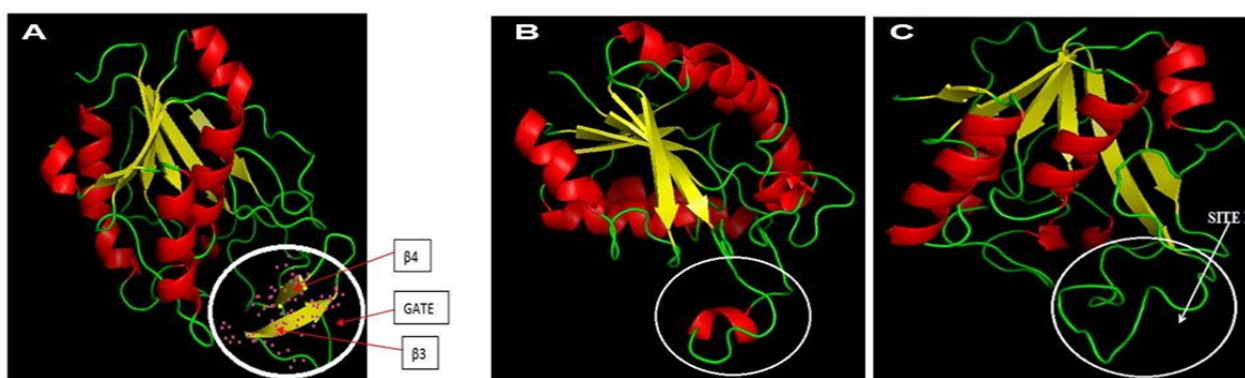
Using the 3D structures of PZase from seven different species, binding site of the enzymes were predicted by means of Q-SiteFinder, Pocket-Finder and SiteMap and residues present in the binding sites were enumerated in **Table 1**. In order to generate docking complexes of PZase and PZA, docking grid was set to cover the corresponding binding site residues of each PZase and 100 conformations were generated in each case. The binding energies calculated between PZA and Pzase from *M. tuberculosis*, *M. marinum*, *M. smegmatis*, *M. bovis*, *M. avium*, *M. abscessus* and *M. kansasii* were 5.5 kcal/mol, 5.4 kcal/mol, 4.8 kcal/mol, 4.8 kcal/mol, 4.7 kcal/mol, 4.6 kcal/mol and 4.5 kcal/mol, respectively. These findings imply that the active sites of PZase may not be in positions to account MDR nature of the PZases from different species of *Mycobacterium*.

**Table 1: Predicted binding site residues of PZases from various species of *Mycobacterium*.**

S. No.	Species Name	Residues
1.	<i>M. abscessus</i>	D9, F14, D49, K96, I133, A134, Y137, C138
2.	<i>M. avium</i>	D8, F13, D50, H72, Y104, I134, A135, H138, C139
3.	<i>M. bovis</i>	D8, F13, D49, K96, I133, A135, H137, C138
4.	<i>M. kansasii</i>	D8, F13, D49, H57, H71, V133, A134, H137, C138
5.	<i>M. marinum</i>	V7, D8, F13, D49, K96, V133, A134, C138, I163
6.	<i>M. smegmatis</i>	D8, F13, D49, H57, K96, Y103, I133, A134, Y137, C138
7.	<i>M. tuberculosis</i>	D8, F13, D49, I133, A134, H137, C138

**Table 2: Analyses of binding sites of PZases from various *Mycobacterium* species.**

Species	Volume (Å <sup>3</sup> )	Surface (Å <sup>2</sup> )	Lipo surface (Å <sup>2</sup> )	Depth (Å)
<i>M. abscessus</i>	702.21	1197.31	771.96	17.76
<i>M. avium</i>	769.98	1413.05	989.66	20.15
<i>M. bovis</i>	670.02	1173.51	712.15	16.80
<i>M. kansasii</i>	470.46	764.33	503.64	13.66
<i>M. marinum</i>	597.18	1059.06	634.14	15.18
<i>M. smegmatis</i>	633.28	916.04	730.91	16.42
<i>M. tuberculosis</i>	505.09	756.15	582.44	18.08


**Figure 2: ‘GATE’ regions of A) *AbPncA*, B) *SpNic* and C) counterpart region of *MtPncA* are indicated by white circles.**

### 3.3 Binding sites architectures and ‘GATE’ analyses

Structural architectures of binding sites of Pzases from different species of *Mycobacterium* were probed by using DoGSiteScorer and the properties such as overall volume, total surface, lipo surface and average depth are listed out in **Table 2**. However, the data were not very helpful to tackle differences among the species towards PZA resistances. For instance, *M. avium*, one of the resistant species, showed active site depth value of 20.2 Å and the value was found to be higher than that of susceptible *M. tuberculosis*. Moreover, values for active sites depth of all seven species were comparable to each other suggesting that analyses on structural architectures of binding sites of PZases were inconclusive on accounting MDR nature of the PZases from different species of *Mycobacterium*.

In these backgrounds, we started our investigation on ‘GATE’ regions that may present in PZases of *Mycobacterium*. In general, ‘GATE’ may help to keep the active sites of proteins either in ‘open state’ or in ‘closed state’ depending upon its conformational orientations. For instance, when the ‘GATE’ opens to external environments, the binding interaction between ligands and proteins may probably be weakened. In contrary, the ‘GATE’ may prefer closed state in order to strengthen the interaction between ligands and protein and the state may

also help to lessen the exoteric effect on the proteins – ligands complexes. **Figure 2** shows the ‘GATE’ regions present in proteins such as *Acinetobacter baumannii* PncA (*AbPncA*) and *Streptococcus pneumoniae* Nicotinamidase (*SpNic*):  $\beta$ -sheets and an  $\alpha$ -helix act as ‘GATE’ region in *AbPncA* and *SpNic*, respectively. Strikingly, the kind of ‘GATE’ region was absent in *Mycobacterium tuberculosis* PncA (*MtPncA*) as shown in Fig. 2 and PZases from other *Mycobacterium* species considered in the present study were also bereft of the ‘GATE’ regions regulating their active sites. The data suggested that the PZase – PZA interactions are probably liable to be disrupted by solvent owing to the absence of the “GATE” regions in the enzymes. This hypothesis was also confirmed by performing molecular dynamics (MD) simulations of all PZases – PZA complexes at 310 K and as well at 373 K in the presence of water models at pH 7.0. The MD data analyses suggested that the PZA started to leave out of the active sites of PZases studied in the present study in the time span of 2500 ps (data not shown). More detailed studies on understanding the structural interactions between PZases and PZA complexes and thermodynamic stabilities of the complexes are right now under progress in our laboratory.

#### 4. CONCLUDING REMARKS

Pyrazinamidase sequences of various species of *Mycobacterium* have been retrieved from protein primary database. The three-dimensional structures of pyrazinamidases from *M. abscessus*, *M. avium*, *M. kansasii*, *M. bovis*, *M. marinum*, and *M. smegmatis* have been homology modeled and the modeled structures have also been thoroughly validated using SAVES meta server. All the pyrazinamidases structures have been subjected to molecular dynamic simulations at close quarters of physiological conditions (pH 7.0, 310 K and 0.1M NaCl) and the resultant dynamic structures were used for analysing structural architectures and also for predicting surface grooves of the enzymes. The binding sites of the pyrazinamidases have been predicted using an array of online and offline computational tools. The binding sites were then used for setting up grids for docking studies performed between PZA and PZases. However, the binding energies obtained for PZA – PZase from *M. tuberculosis*, which is susceptible to PZA and for PZA - PZases from other six PZA-resistant species were found to be comparable to each other. Comprehensive analyses on overall volumes, average depths and structural architectures of the binding sites of the PZases were also inconclusive to figure-out the mechanism of the PZases resistance towards PZA. It seems that the sizes and shapes of active sites of the enzymes have no or negligible effect on their activities. Interestingly, either bereft of ‘GATE’ region or ‘ill-formed GATE’ regions of PZases as demonstrated in the present study may act as probable structural factors for the differential binding affinities of the pyrazinamidase variants towards the interaction with pyrazinamide and as well PZA-resistant properties of the enzymes.

#### REFERENCES

- [1] Wallis, R. S., Jakubiec, W., Mitton-Fry, M., Ladutko, L., Campbell, S., Paige, D., Silvia, A., Miller, P. F., *PLoS ONE* 2012, 7(1), e30479.
- [2] Raman, K., Chandra, N., *BMC Microbiol.* 2008, 8, 234.
- [3] Juréen, P., Werngren, J., Toro, J.-C., Hoffner, S., *Antimicrob. Agents Chemother.* 2008, 52(5), 1852–1854.
- [4] Scorpio, A., Zhang, Y., *Nat. Med.(N.Y.)*. 1996, 2, 662 – 667.
- [5] Konno, K., Feldmann, F. M., McDermott, W., *Am. Rev. Respir. Dis.* 1967, 95, 461 – 469.
- [6] Agrawal, S., Singh, I., Kaur, K. J., Bhade, S. R., Kaul C. L., Panchagnula, R., *Int. J. Pharm.* 2004, 276(1-2), 41 – 49.
- [7] Wade, M.M., Zhang, Y., *J. Med. Microbiol.* 2004, 53(8), 769 – 773.
- [8] Daniel, J., Maamar, H., Deb, C., Sirakova, T. D., Kolattukudy, P. E., *PLoS Pathogens.* 2011, 7(6), e1002093.
- [9] Medjahed, H., Gaillard, J.-L., Reyat, J.-M., *Trends Microbiol.* 2010, 18(3), 117 – 123.
- [10] Lety, M. A., Nair, S., Berche, P., Escuyer, V., *Antimicrob. Agents Chemother.* 2005, 41(12), 2629 – 2633.
- [11] Sun, Z., Zhang, Y., *Antimicrob. Agents Chemother.* 1999, 43(3), 537 – 542.
- [12] Petrella, S., Gelus-Ziental, N., Maudry, A., Laurans, C., Boudjelloul, R., Sougakoff, W., *PLoS ONE.* 2011, 6(1), e15785.
- [13] Zhang, J.-L., Zheng, Q.-C., Li, Z.-Q., Zhang, H.-X., *PLoS ONE.* 2012, 7(6), e39546.
- [14] Sali, A., Blundell, T. L., *J. Mol. Biol.* 1993, 234, 779–815.
- [15] Berendsen, H.J.C., van der Spoel, D., van Drunen, R., *J. Chem. Theory Comput.* 1995, 8, 3207–3216.
- [17] Brooks, B. R., Bruccoleri, R. E., Olafson, B. D., States, D. J., Swaminathan, S., Karplus, M., *J. Comp. Chem.* 1983, 4(2), 187–217.
- [18] Zoete, V., Cuendet, M. A., Grosdidier, A., Michielin, O., *J. Comput. Chem.* 2011, 32(11), 2359 – 2368.
- [19] Laurie, A. T., Jackson, R. M., *Bioinformatics* 2005, 21(9), 1908 – 1916.
- [20] Volkamer, A., Kuhn, D., Rippmann, F., Rarey, M., *Bioinformatics* 2012, 28(15), 2074 – 2075.
- [21] Morris, G. M., Goodsell, D. S., Halliday, R.S., Huey, R., Hart, W. E., Belew, R. K., Olson, A. J., *J. Computational Chemistry* 1998, 19, 1639 – 1662.